Nonlinear waves of the Hirota and the Maxwell–Bloch equations in nonlinear optics*

Li Chuan-Zhong(李传忠)[a], He Jing-Song(贺劲松)[a]†, and K. Porsezian[b,c]

[a] *Department of Mathematics, Ningbo University, Ningbo* 315211, *China*
[b] *Department of Physics, Pondicherry University, Puducherry* 605014, *India*
[c] *Institute of Condensed Matter Theory and Solid State Optics, Friedrich–Schiller-Universität Jena, Max-Wein Platz 1, D-*07743 *Jena, Germany*

(Received 25 August 2012; revised manuscript received 24 September 2012)

In this paper, considering the Hirota and the Maxwell–Bloch (H-MB) equations which are governed by femtosecond pulse propagation through a two-level doped fiber system, we construct the Darboux transformation of this system through a linear eigenvalue problem. Using this Daurboux transformation, we generate multi-soliton, positon, and breather solutions (both bright and dark breathers) of the H-MB equations. Finally, we also construct the rogue wave solutions of the above system.

Keywords: Hirota and Maxwell–Bloch equations, nonlinear optics, rogue wave

PACS: 42.65.Tg, 42.65.Sf, 05.45.Yv, 02.30.Ik **DOI:** 10.1088/1674-1056/22/4/044208

1. Introduction

In the recent past, nonlinear integrable systems have attracted a lot of attention among researchers. This fascinating subject of nonlinear science has branched out in almost all areas of science and technology. Its applications are expanding through the whole of physics from hydrodynamics to nonlinear optics, plasma physics, elementary particle physics, etc. In general, nonlinear phenomena are often modeled by nonlinear evolution equations exhibiting a wide range of high complexities. In recent years, the advent of high-speed computers, advanced software, and development of many sophisticated analytical methods in the study of the nonlinear phenomena have encouraged both the theory and experiment. Due to various developments in this fast-growing area, nonlinear science has experienced an explosive growth through the invention of several exciting new technologically possible concepts like solitons, dromions, rogue waves, similaritons, supercontinuum generation, complete integrability, fractals, chaos, and so on.[1–10] In particular, many new exciting developments have been reported by several groups in different physical systems with suitable nonlinear effects. Though the concept of solitons have been observed in many of the integrable systems through both analytical and experimental methods, in recent years, new concepts like similaritons and rogue waves have also attracted considerable attention in many nonlinear physical systems.[1,4–10] Among all the concepts, rogue waves have also not only been the subject of intensive research in oceanography (Refs. [11]–[15]), but observed in several other areas, such as Bose–Einstein condensate,[16,17] surface and space plasma,[18,19] financial rogues wave describing the possible physical mechanisms in financial markets and related fields,[20] and superfluids.[21,22] In optics, they were observed when propagating high power optical radiation through photonic crystal fiber.[23,24] Moreover several soliton equations, such as the nonlinear Schrödinger (NLS) equation,[25] the Hirota equation,[26,27] the first type derivative NLS equation,[28] the third type DNLS equation,[29] the discrete NLS equation,[30] the two-component NLS equations,[31–33] nad high order NLS equations[34] admit rogue waves.

In 1973, Hasegawa and Tappert[35] modeled the propagation of optical soliton pulses in nonlinear fibers through the derivation of the NLS equation without loss. To compensate the loss in transmission systems, nowadays repeaters are placed at periodic intervals to provide necessary amplification and reshaping of the pulses. The problem of loss can be handled with either Raman amplification or amplification through continuous wave pumping in erbium-doped fibers.[1] However, with doping of two-level resonant impurity atoms like erbium (Er), one can achieve the so-called self-induced transparency (SIT) phenomenon in fibers. Actually the SIT effect is also a soliton effect in a two-level resonant medium. So in addition to the optical soliton SIT, solitons can also be achieved in Er-doped fibers. This can almost solve the major constraints in the transmission of long-distance fiber optic communication.

In 1967, McCall and Hahn[36] invented the remarkable coherent pulse propagation in two-level resonant media, which can be explained by using Maxwell–Bloch (MB) equations. The coherent absorption takes place and the medium becomes optically transparent to that particular wavelength when the energy difference between the two-levels of the media coin-

*Project supported by the Natural Science Foundation of Zhejiang Province of China (Grant No. LY12A01007), the National Natural Science Foundation of China (Grant Nos. 11201251, 10971109, and 11271210), K. C. Wong Magna Fund in Ningbo University, and K. Porseizan wishes to thank the DST, DAE-BRNS, UGC, and CSIR, Government of India, for the financial support through major projects.

†Corresponding author. E-mail: hejingsong@nbu.edu.cn

© 2013 Chinese Physical Society and IOP Publishing Ltd

cides with the optical wavelength. SIT can also be induced in optical fibers when the fibers are doped with erbium atoms. This was shown by Maimistov and Manykin in 1983.[37] The system will be governed by the coupled system of the NLS equation and the MB equation (NLS-MB equations) if we consider these effects for a large width pulse. The coexistence of NLS solitons and SIT solitons in erbium-doped resonant fibers was experimentally observed by Nakazawa *et al.*[38,39] Recently, multi-soliton solutions of the coupled NLS-MB equation were shown in Ref. [40]. In Ref. [41], the periodic solutions of the coupled NLS-MB equation have been generated through Darboux transformation and later its rogue wave solutions were derived from the breather solution in Ref. [42].

For high bit rate transmission, it has been well proved that many higher-order effects such as higher-order dispersion, self-steepening, and stimulated inelastic scattering have to be included in the governing model. All these higher-order effects are usually treated as perturbation to the NLS system. With the inclusion of all the above higher-order effects, the possibility of exact soliton-type pulse propagation in optical fibers has been reported by many authors. Many interesting experimental and theoretical results were also reported in favor of optical solitons for its usage in futuristic high speed optical communication. The HNLS-MB equations as a higher-order correction of NLS-MB equations was shown to allow soliton-type pulse propagation under a particular parametric condition.[43,44]

Kodama[45] has shown that with suitable transformation and omitting the higher-order terms, the higher-order nonlinear Schrödinger equation can be reduced to the Hirota equation.[46] For the generalized Hirota equation with variable coefficients, one can find the effect of a dispersion tailored profile and optimal amplification through dispersion wells and barriers on femtosecond soliton propagation.[47] After a suitable choice of self-steepening and self-frequency effects, the HNLS-MB equations can be reduced to a coupled system of the Hirota equation and the MB equation in the following form[48]

$$E_z = \mathrm{i}\alpha(\frac{1}{2}E_{tt} + |E|^2E) + \beta(E_{ttt} + 6|E|^2E_t) + 2p, \quad (1)$$

$$p_t = 2\mathrm{i}\omega p + 2E\eta, \quad (2)$$

$$\eta_t = -(Ep^* + E^*p), \quad (3)$$

where E is the normalized slowly varying amplitude of the complex field envelope, p is the polarization, η means population inversion, (ω, α, β) are three real constants and $*$ represents complex conjugate. The H-MB system has been shown to be integrable and also admits the Lax pair and other required properties for complete integrability.[48] Specifically, its Lax pair is expressed in the form of the linear eigenvalue problem

$$\Phi_t = U\Phi, \quad \Phi_z = V\Phi, \quad (4)$$

where

$$U = \lambda\begin{pmatrix} -\mathrm{i} & 0 \\ 0 & \mathrm{i} \end{pmatrix} + \begin{pmatrix} 0 & E \\ -E^* & 0 \end{pmatrix} = -\mathrm{i}\lambda\sigma_3 + U_0, \quad \sigma_3 = \begin{pmatrix} 1 & 0 \\ 0 & -1 \end{pmatrix}, \quad (5)$$

$$V = \lambda^3\begin{pmatrix} 4\mathrm{i}\beta & 0 \\ 0 & -4\mathrm{i}\beta \end{pmatrix} + \lambda^2\begin{pmatrix} -\alpha\mathrm{i} & -4\beta E \\ 4\beta E^* & \alpha\mathrm{i} \end{pmatrix} + \lambda\begin{pmatrix} -2\beta\mathrm{i}|E|^2 & \alpha E - 2\beta\mathrm{i}E_t \\ -\alpha E^* - 2\beta\mathrm{i}E_t^* & 2\beta\mathrm{i}|E|^2 \end{pmatrix}$$
$$+ \begin{pmatrix} \frac{\alpha}{2}\mathrm{i}|E|^2 - \beta(EE_t^* - E_tE^*) & 2\beta|E|^2E + \frac{\alpha}{2}\mathrm{i}E_t + \beta E_{tt} \\ -2\beta|E|^2E^* + \frac{\alpha}{2}\mathrm{i}E_t^* - \beta E_{tt}^* & -\frac{\alpha}{2}\mathrm{i}|E|^2 + \beta(EE_t^* - E_tE^*) \end{pmatrix} + \mathrm{i}\frac{1}{\lambda+\omega}\begin{pmatrix} \eta & -p \\ -p^* & -\eta \end{pmatrix}. \quad (6)$$

We can get the classical Hirota and the Maxwell–Bloch system when $\alpha = 2, \beta = -1$.

It is well known that the Darboux transformation is one of the effective methods to generate the soliton solutions for integrable equations.[49] The main task of this paper will be to construct different kinds of solutions of the H-MB equations by this method. The one-fold and two-folds Darboux transformation are constructed. Further, one-soliton, two-soliton, and positons are derived by assuming a trivial seed solution by the Darboux transformation. Then starting from a periodic seed solution, breather solutions of the H-MB equations are also constructed. Finally, the Taylor expansion of these breather solutions will be used to construct the rogue wave solution.

2. Darboux transformation of the H-MB equation

Using the linear eigenvalue equations of H-MB equations, we have constructed the n-folds Darboux transformation. The details of deriving Darboux transformation is too tedious to write here. We just focus on the dynamical evolution of the solutions generated by one-fold and two-folds Darboux transformations in this section. For this purpose, we introduce 4 eigenfunctions

$$\begin{pmatrix} \Phi_{1,i} \\ \Phi_{2,i} \end{pmatrix} = \Phi_{\lambda=\lambda_i}, \ i = 1,2,3,4 \quad (7)$$

with the following constraint on the eigenvalues $\lambda_{2i-1} = \lambda_{2i}^*$ and the reduction conditions on eigenfunctions as $\Phi_{2,2i} = \Phi_{1,2i-1}^*$ and $\Phi_{2,2i-1} = -\Phi_{1,2i}^*$.

The determinant representations of one-fold and two-folds Darboux transformations of the H-MB equations will be introduced in the following two propositions using the same technique in Ref. [50].

Proposition 1 The one-fold Darboux transformation of the H-MB equations is as follows:

$$E^{[1]} = E + 2\mathrm{i}\frac{(T_1)_{12}}{\Delta_1}, \tag{8}$$

$$p^{[1]} = \frac{2\eta(T_1)_{11}(T_1)_{12} - p^*(T_1)_{12}(T_1)_{12} + p(T_1)_{11}(T_1)_{11}}{(T_1)_{11}(T_1)_{22} - (T_1)_{12}(T_1)_{21}}\Big|_{\lambda=-\omega}, \tag{9}$$

$$\eta^{[1]} = \frac{\eta((T_1)_{11}(T_1)_{22} + (T_1)_{12}(T_1)_{21}) - p^*(T_1)_{12}(T_1)_{22} + p(T_1)_{11}(T_1)_{21}}{(T_1)_{11}(T_1)_{22} - (T_1)_{12}(T_1)_{21}}\Big|_{\lambda=-\omega}, \tag{10}$$

where

$$\Delta_1 = \begin{vmatrix} \Phi_{1,1} & \Phi_{2,1} \\ \Phi_{1,2} & \Phi_{2,2} \end{vmatrix}, \tag{11}$$

$$(\mathbb{T}_1)_{11} = \begin{vmatrix} 1 & 0 & \lambda \\ \Phi_{1,1} & \Phi_{2,1} & \lambda_1\Phi_{1,1} \\ \Phi_{1,2} & \Phi_{2,2} & \lambda_2\Phi_{1,2} \end{vmatrix}, \quad (\mathbb{T}_1)_{12} = \begin{vmatrix} 0 & 1 & 0 \\ \Phi_{1,1} & \Phi_{2,1} & \lambda_1\Phi_{1,1} \\ \Phi_{1,2} & \Phi_{2,2} & \lambda_2\Phi_{1,2} \end{vmatrix}, \tag{12}$$

$$(\mathbb{T}_1)_{21} = \begin{vmatrix} 1 & 0 & 0 \\ \Phi_{1,1} & \Phi_{2,1} & \lambda_1\Phi_{2,1} \\ \Phi_{1,2} & \Phi_{2,2} & \lambda_2\Phi_{2,2} \end{vmatrix}, \quad (\mathbb{T}_1)_{22} = \begin{vmatrix} 0 & 1 & \lambda \\ \Phi_{1,1} & \Phi_{2,1} & \lambda_1\Phi_{2,1} \\ \Phi_{1,2} & \Phi_{2,2} & \lambda_2\Phi_{2,2} \end{vmatrix}. \tag{13}$$

Proposition 2 The two-folds Darboux transformation of H-MB equations is

$$E^{[2]} = E + 2\mathrm{i}(t_1^{[2]})_{12}, \tag{14}$$

$$p^{[2]} = \frac{2\eta(T_2)_{11}(T_2)_{12} - p^*(T_2)_{12}(T_2)_{12} + p(T_2)_{11}(T_2)_{11}}{(T_2)_{11}(T_2)_{22} - (T_2)_{12}(T_2)_{21}}\Big|_{\lambda=-\omega}, \tag{15}$$

$$\eta^{[2]} = \frac{\eta((T_2)_{11}(T_2)_{22} + (T_2)_{12}(T_2)_{21}) - p^*(T_2)_{12}(T_2)_{22} + p(T_2)_{11}(T_2)_{21}}{(T_2)_{11}(T_2)_{22} - (T_2)_{12}(T_2)_{21}}\Big|_{\lambda=-\omega}, \tag{16}$$

where

$$(t_1^{[2]})_{12} = \frac{1}{\Delta_2}\begin{vmatrix} \Phi_{1,1} & \Phi_{2,1} & \lambda_1\Phi_{1,1} & \lambda_1^2\Phi_{1,1} \\ \Phi_{1,2} & \Phi_{2,2} & \lambda_2\Phi_{1,2} & \lambda_2^2\Phi_{1,2} \\ \Phi_{1,3} & \Phi_{2,3} & \lambda_3\Phi_{1,3} & \lambda_3^2\Phi_{1,3} \\ \Phi_{1,4} & \Phi_{2,4} & \lambda_4\Phi_{1,4} & \lambda_4^2\Phi_{1,4} \end{vmatrix}, \qquad \Delta_2 = \begin{vmatrix} \Phi_{1,1} & \Phi_{2,1} & \lambda_1\Phi_{1,1} & \lambda_1\Phi_{2,1} \\ \Phi_{1,2} & \Phi_{2,2} & \lambda_2\Phi_{1,2} & \lambda_2\Phi_{2,2} \\ \Phi_{1,3} & \Phi_{2,3} & \lambda_3\Phi_{1,3} & \lambda_3\Phi_{2,3} \\ \Phi_{1,4} & \Phi_{2,4} & \lambda_4\Phi_{1,4} & \lambda_4\Phi_{2,4} \end{vmatrix}, \tag{17}$$

$$(\mathbb{T}_2)_{11} = \begin{vmatrix} 1 & 0 & \lambda & 0 & \lambda^2 \\ \Phi_{1,1} & \Phi_{2,1} & \lambda_1\Phi_{1,1} & \lambda_1\Phi_{2,1} & \lambda_1^2\Phi_{1,1} \\ \Phi_{1,2} & \Phi_{2,2} & \lambda_2\Phi_{1,2} & \lambda_2\Phi_{2,2} & \lambda_2^2\Phi_{1,2} \\ \Phi_{1,3} & \Phi_{2,3} & \lambda_3\Phi_{1,3} & \lambda_3\Phi_{2,3} & \lambda_3^2\Phi_{1,3} \\ \Phi_{1,4} & \Phi_{2,4} & \lambda_4\Phi_{1,4} & \lambda_4\Phi_{2,4} & \lambda_4^2\Phi_{1,4} \end{vmatrix}, \quad (\mathbb{T}_2)_{12} = \begin{vmatrix} 0 & 1 & 0 & \lambda & 0 \\ \Phi_{1,1} & \Phi_{2,1} & \lambda_1\Phi_{1,1} & \lambda_1\Phi_{2,1} & \lambda_1^2\Phi_{1,1} \\ \Phi_{1,2} & \Phi_{2,2} & \lambda_2\Phi_{1,2} & \lambda_2\Phi_{2,2} & \lambda_2^2\Phi_{1,2} \\ \Phi_{1,3} & \Phi_{2,3} & \lambda_3\Phi_{1,3} & \lambda_3\Phi_{2,3} & \lambda_3^2\Phi_{1,3} \\ \Phi_{1,4} & \Phi_{2,4} & \lambda_4\Phi_{1,4} & \lambda_4\Phi_{2,4} & \lambda_4^2\Phi_{1,4} \end{vmatrix},$$

$$(\mathbb{T}_2)_{21} = \begin{vmatrix} 1 & 0 & \lambda & 0 & 0 \\ \Phi_{1,1} & \Phi_{2,1} & \lambda_1\Phi_{1,1} & \lambda_1\Phi_{2,1} & \lambda_1^2\Phi_{2,1} \\ \Phi_{1,2} & \Phi_{2,2} & \lambda_2\Phi_{1,2} & \lambda_2\Phi_{2,2} & \lambda_2^2\Phi_{2,2} \\ \Phi_{1,3} & \Phi_{2,3} & \lambda_3\Phi_{1,3} & \lambda_3\Phi_{2,3} & \lambda_3^2\Phi_{2,3} \\ \Phi_{1,4} & \Phi_{2,4} & \lambda_4\Phi_{1,4} & \lambda_4\Phi_{2,4} & \lambda_4^2\Phi_{2,4} \end{vmatrix}, \quad (\mathbb{T}_2)_{22} = \begin{vmatrix} 0 & 1 & 0 & \lambda & \lambda^2 \\ \Phi_{1,1} & \Phi_{2,1} & \lambda_1\Phi_{1,1} & \lambda_1\Phi_{2,1} & \lambda_1^2\Phi_{2,1} \\ \Phi_{1,2} & \Phi_{2,2} & \lambda_2\Phi_{1,2} & \lambda_2\Phi_{2,2} & \lambda_2^2\Phi_{2,2} \\ \Phi_{1,3} & \Phi_{2,3} & \lambda_3\Phi_{1,3} & \lambda_3\Phi_{2,3} & \lambda_3^2\Phi_{2,3} \\ \Phi_{1,4} & \Phi_{2,4} & \lambda_4\Phi_{1,4} & \lambda_4\Phi_{2,4} & \lambda_4^2\Phi_{2,4} \end{vmatrix}.$$

With these two Darboux transformations mentioned above, soliton and positon solutions of the H-MB equation will be derived in the next section.

3. Soliton and positon solutions of the H-MB equations

Firstly, we will consider the construction of a one-soliton solution of the H-MB equations by assuming a seed solution $E = 0$, $p = 0$, $\eta = 1$ in Proposition 1. After setting $\lambda = \alpha_1 + \beta_1\mathrm{i}$ in Eqs. (8)–(10), the one-solition solution is obtained. Further, if we choose $\alpha = 1$, $\beta = 0$, our one-soliton solution is reduced to the soliton solution of NLS-MB equations reported in Ref. [40] by a transformation $\alpha_1 = -\rho_1$, $\beta_1 = \nu_1$. Similarly, after substituting two eigenfunctions into the Darboux transformation equation and taking $\alpha = 2$, $\beta = -1$, we can obtain the one-solition solutions of the classical H-MB equations whose evolution is given in Fig. 1.

For the purpose of construction of two-soliton solutions, we use two spectral parameters namely $\lambda_1 = \alpha_1 + \beta_1\mathrm{i}$ and $\lambda_2 = \alpha_2 + \beta_2\mathrm{i}$ in Proposition 2. As the general form of the two-soliton solution is tedious in nature, for simplicity, we only give the pictures of the two-soliton solution with the following choice of parameters $\omega = 1$, $\alpha_1 = 2$, $\beta_1 = 1$, $\alpha_2 = 1$, $\beta_2 = 2$, $\alpha = 2$, $\beta = -1$ in Fig. 2.

Now we can consider the bright and dark positon solutions of the H-MB equation. In the above constructed two-soliton solutions, if we choose the second spectral parameter λ_2 to be close to the first spectral parameter λ_1 and do the Taylor expansion of the wave function to the first order up to λ_1, it will lead to a new kind of positon solutions. Now we take $\lambda_2 = \lambda_1 + \varepsilon(1+\mathrm{i})$ and use the Taylor expansion of wave function ϕ_3 and ϕ_4 up to the first order of ε in terms of λ_1. For example, after taking values as $\omega = 1$, $\alpha_1 = 2$, $\beta_1 = 1$, $\alpha = 2$, $\beta = -1$, the positon solution E is constructed in the form

$$E_{\rm p} = -40{\rm i}\exp\Big(-\frac{137}{5}{\rm i}z - 4{\rm i}t\Big)\frac{(20t+3998z-30{\rm i})\cosh\Big(\frac{521}{5}z+2t\Big)+(60{\rm i}t+1606{\rm i}z)\sinh\Big(\frac{521}{5}z+2t\Big)}{50+400t^2+1856324z^2+35264tz+50\cosh\Big(\frac{1042}{5}z+4t\Big)}.$$

A pictorial representation of positon solutions of the H-MB equations is shown in Fig. 3.

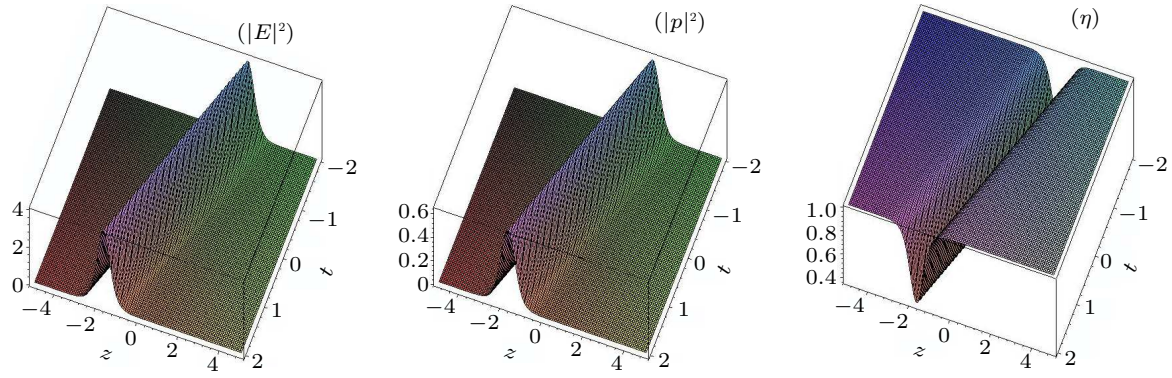


Fig. 1. (color online) One-solition solution (E, p, η) of the H-MB equations when $\omega = 1.5$, $\alpha_1 = 0.5$, $\beta_1 = 1$, $\alpha = 2$, $\beta = -1$.

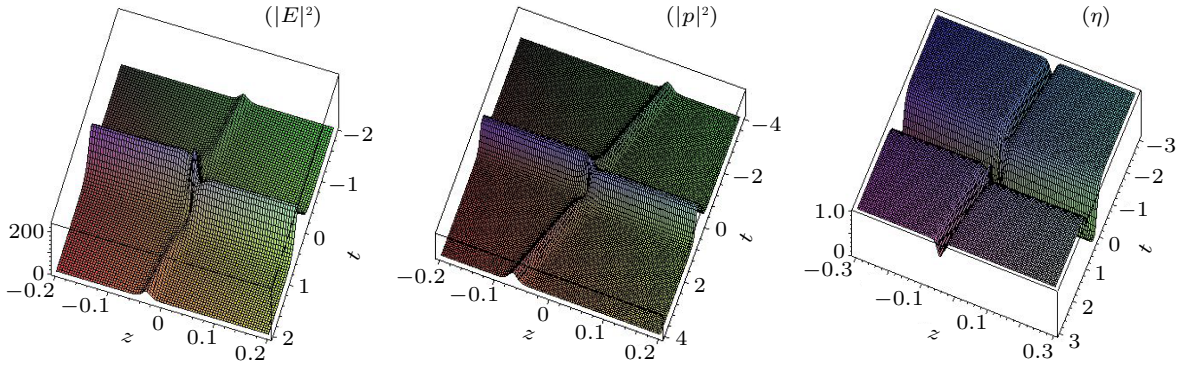


Fig. 2. (color online) Two-solition solution (E, p, η) of the H-MB equations when $\omega = 1$, $\alpha_1 = 2$, $\beta_1 = 1$, $\alpha_2 = 1$, $\beta_2 = 2$, $\alpha = 2$, $\beta = -1$.

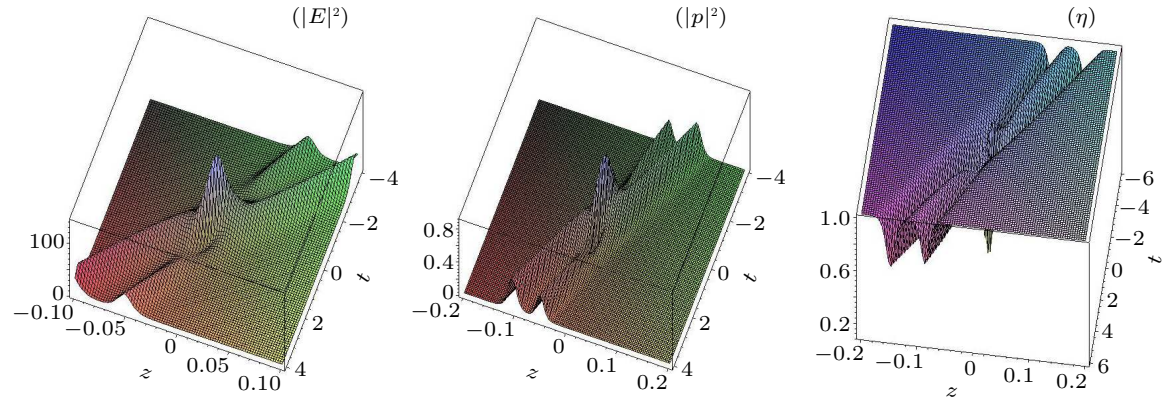


Fig. 3. (color online) One positon solution (E, p, η) of the H-MB equations when $\omega = 1$, $\alpha_1 = 2$, $\beta_1 = 1$, $\alpha = 2$, $\beta = -1$.

4. Bright and dark breather solutions

So far, solitons and positons solutions for H-MB equations have been generated. These solutions have been obtained through Darboux transformation by assuming constant trivial solutions. In this section, being different from solitons and positons, we will now focus on a new kind of solution which is derived from periodic solutions through Darboux transformation. The resulting periodic solutions can be called breather solutions.

Taking a periodic seed solution $E = d\,{\rm e}^{{\rm i}\rho}$, $p = {\rm i}fE$,

$\eta = 1$, $\rho = az + bt$ into in Eqs. (8)–(10), which admits the constraint in the form

$$2a + \alpha b^2 - 2\alpha d^2 + 2\beta b^3 - 12\beta d^2 b - 4f = 0,$$
$$fb - 2\omega f + 2 = 0. \tag{18}$$

To simplify the calculations, we take $b = -2\alpha_1$ and use the Darboux transformation in Proposition 1. Then the final form of breather solutions can be obtained. Now, taking $\omega = 0.5$, $d = 0.5$, $n_1 = 1$, $\alpha_1 = -1$, $\beta_1 = 1$, $t = z = 1$, the above breather solution will lead to the following form of E denoted as $E_{b\alpha\beta}$,

$$\begin{aligned} E_{b\alpha\beta} \;=\; & -0.8\times 10^{-8}\big(435256351\,\mathrm{e}^{-0.3058103975\times 10^{-10}\mathrm{i}(-20605080800-516156736900\beta+586938589\alpha)} \\ & +2243649\,\mathrm{e}^{-0.3058103975\times 10^{-8}\mathrm{i}(3258050808+8431567369\beta+1138630614\alpha)} \\ & -62500000\,\mathrm{e}^{0.3058103975\times 10^{-8}\mathrm{i}(-1635000000\beta-572250000\alpha+1132761229i\alpha-1526000000-1085995856\mathrm{i}+4247854606\mathrm{i}\beta)} \\ & -62500000\,\mathrm{e}^{-0.3058103975\times 10^{-8}\mathrm{i}(1635000000\beta+572250000\alpha+1132761229i\alpha+1526000000-1085995856\mathrm{i}+4247854606\mathrm{i}\beta)}\big) \\ & /\big(\cos(1.732050807\alpha+20.78460969\beta+5.29679146)-2\cosh(12.99038106\beta-3.321088245+3.464101615\alpha)\big). \end{aligned}$$

For example, after taking values

$$\omega = 0.7, d = 0.5, n_1 = 1.2, \alpha_1 = -1,$$
$$\beta_1 = 1, \alpha = 2, \beta = -1, \tag{19}$$

i.e., the case of H-MB equations, the breather solution of E is included in Fig. 4 and its corresponding density graph is shown in Fig. 5.

To understand the above results, choosing the values as $\omega = 0.7$, $d = 0.5$, $n_1 = 1.2$, $\alpha_1 = -1$, $\beta_1 = 0.6$, $\alpha = 1$, $\beta = 0$, i.e., the case of the NLS-MB equations, the picture of breather solution of the NLS-MB equations is shown in Fig. 6 and its density graph is shown in Fig. 7, which clearly show the change of amplitude with respect to changes in values of t and z. All the above results are in agreement with the results of the breather solutions of NLS-MB equations mentioned in Ref. [42].

For the case of coupled mKdV and Maxwell–Bloch (CMKdV-MB) equations, we choose $\omega = 0.7$, $d = 0.5$, $n_1 = 1.2$, $\alpha_1 = -1$, $\beta_1 = 0.6$, $\alpha = 0$, $\beta = 1$. A picture of the breather solutions of the CMKdV-MB equations is portrayed in Fig. 8 and its corresponding density graph is in Fig. 9.

It is interesting to observe that the values of (α, β) also change the direction of breather solution in (t, z) plane.

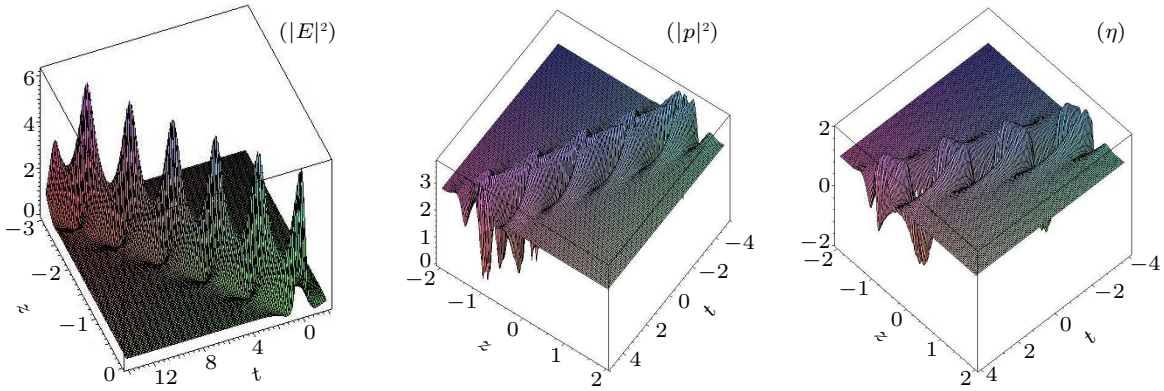


Fig. 4. (color online) Breather solution (E, p, η) of the H-MB equation when $\omega = 0.7$, $d = 0.5$, $n_1 = 1.2$, $\alpha_1 = -1$, $\beta_1 = 1$, $\alpha = 2$, $\beta = -1$.

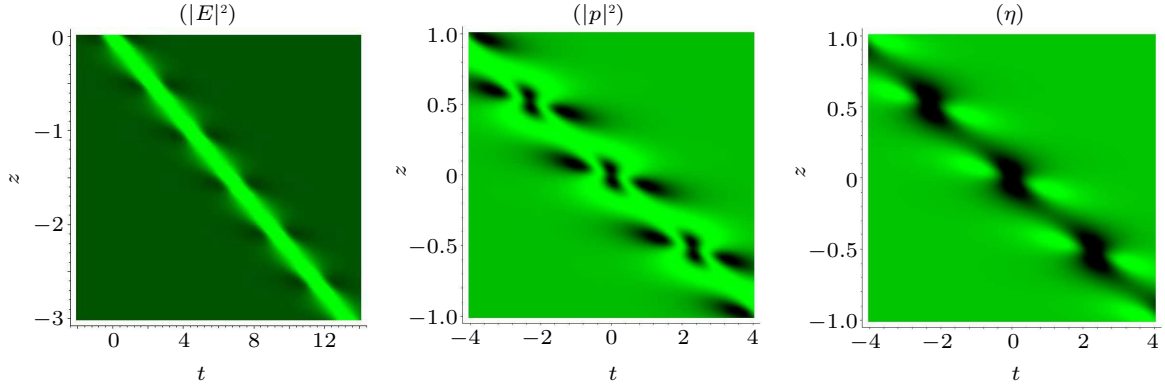


Fig. 5. (color online) Breather solution (E, p, η) of the H-MB equation when $\omega = 0.7$, $d = 0.5$, $n_1 = 1.2$, $\alpha_1 = -1$, $\beta_1 = 1$, $\alpha = 2$, $\beta = -1$.

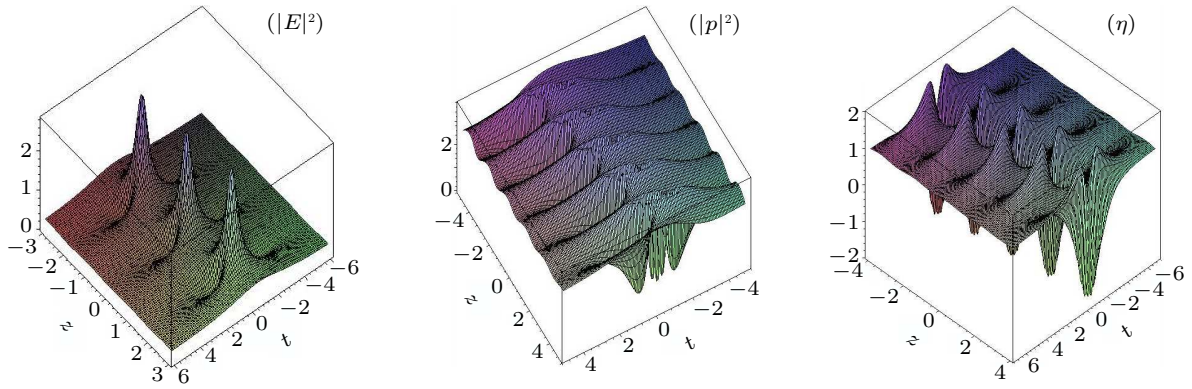


Fig. 6. (color online) Breather solution (E, p, η) of the NLS-MB equations when $\omega = 0.7$, $d = 0.5$, $n_1 = 1.2$, $\alpha_1 = -1$, $\beta_1 = 0.6$, $\alpha = 1$, $\beta = 0$.

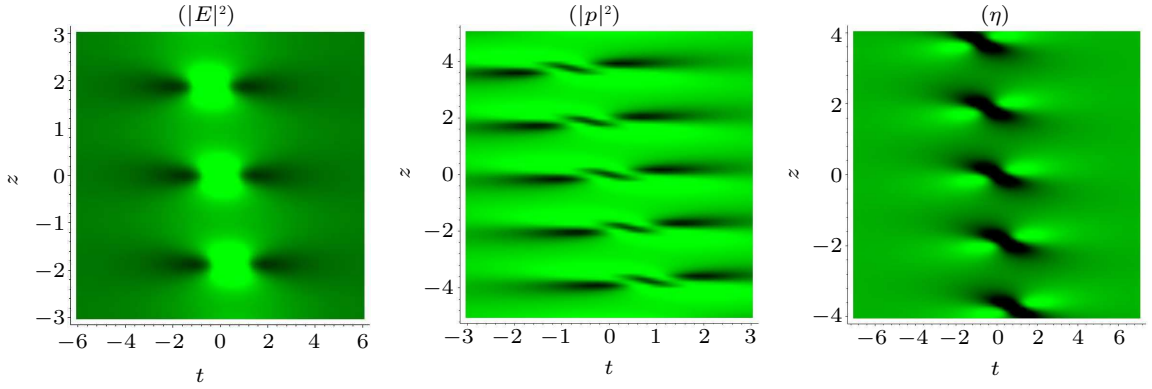


Fig. 7. (color online) Breather solution (E, p, η) of the NLS-MB equations when $\omega = 0.7$, $d = 0.5$, $n_1 = 1.2$, $\alpha_1 = -1$, $\beta_1 = 0.6$, $\alpha = 1$, $\beta = 0$.

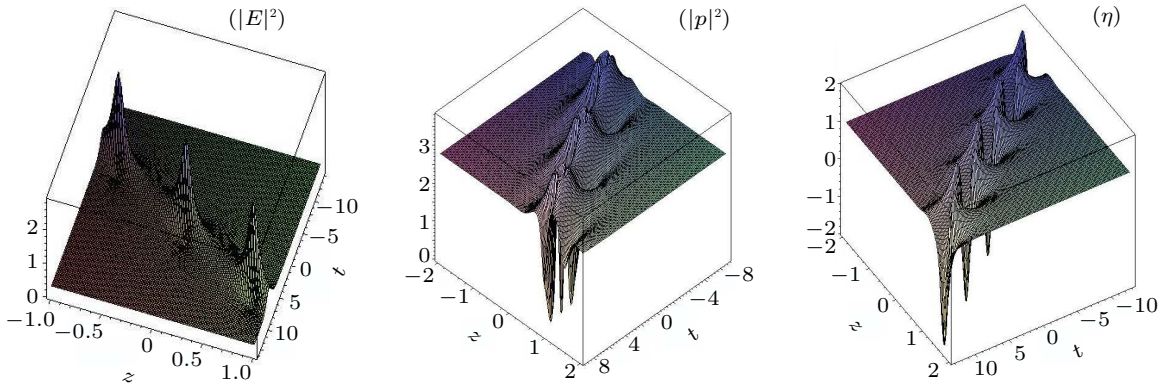


Fig. 8. (color online) Breather solution (E, p, η) of the CMKdV-MB equation when $\omega = 0.7$, $d = 0.5$, $n_1 = 1.2$, $\alpha_1 = -1$, $\beta_1 = 0.6$, $\alpha = 0$, $\beta = 1$.

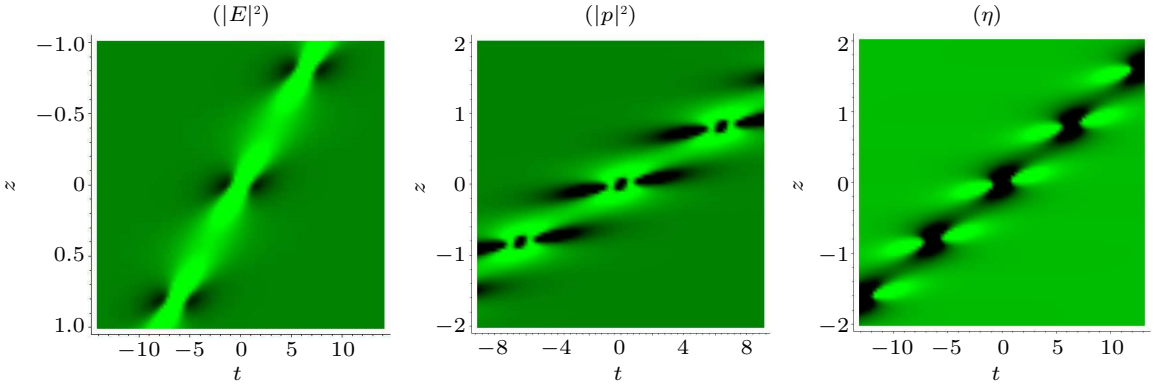


Fig. 9. (color online) Breather solution (E, p, η) of the CMKdV-MB equation when $\omega = 0.7$, $d = 0.5$, $n_1 = 1.2$, $\alpha_1 = -1$, $\beta_1 = 0.6$, $\alpha = 0$, $\beta = 1$.

5. Bright and dark rogue waves

Now, we will concentrate on the construction of the rogue wave solution of H-MB equations. From our careful analysis we conclude that this kind of solution appears only in some special region of time and distance and then will be drawn into one fixed non-vanishing plane. If we do the Taylor expansion of the breather solution around $\beta_1 = d$, one rogue wave solution E_r of E will be obtained and rogue waves for p and η can also be constructed in a similar way. In the following, we report all the rogue wave for (E_r, p_r, η_r) with $\omega = 1, d = 1, n_1 = 1, \alpha_1 = 1, \beta_1 = 1, \alpha = 2, \beta = -1$, the rogue wave is found to be in the form

$$
\begin{aligned}
E_r &= \mathrm{e}^{3\mathrm{i}z-2\mathrm{i}t}\frac{15-5945z^2-408zt-20t^2+556\mathrm{i}z}{5+5945z^2+408zt+20t^2},\\
p_r &= -\frac{1}{2}(3300z+160t-21214\mathrm{i}z^2+35343025\mathrm{i}z^4+226848tz^2+11120t^2z+3305420z^3+400\mathrm{i}t^4\\
&\quad -120\mathrm{i}t^2-55\mathrm{i}+16320\mathrm{i}t^3z+2000\mathrm{i}tz+4851120\mathrm{i}tz^3+404264\mathrm{i}t^2z^2)\,\mathrm{e}^{-\mathrm{i}(-3z+2t)}\\
&\quad \times(25+400t^4+59450z^2+35343025z^4+4851120tz^3+404264t^2z^2+200t^2+4080tz+16320t^3z)^{-1},\\
\eta_r &= 1+\frac{-20-4080tz+4600tz-18476z^2+80t^2}{25+400t^4+35343025z^4+4080tz+4851120tz^3+404264t^2z^2+16320t^3z+59450z^2+200t^2}.
\end{aligned}
$$

The graphical representation on one rogue solution of H-MB equations is shown in Fig. 10.

The density graph corresponding to Fig. 10 is plotted in Fig. 11.

When $\alpha = 1, \beta = 0$, i.e., the NLS-MB equations, the graph of the rogue wave solution is plotted in Fig. 12 from which one can easily find the above-mentioned features for the H-MB equations. The density graph corresponding to Fig. 12 is Fig. 13.

Here again we find that the above solutions also agrees well with the NLS-MB results mentioned in Ref. [42]. To understand the impact of parameters α and β on rogue dynamics, we also consider the case when $\alpha = 0, \beta = 1$, i.e., the CMKdV-MB equations, which can be seen in Fig. 14 and Fig. 15. From the above figures, like in the earlier care, we also find that the parameters α and β change the form of rogue wave structures. Therefore, to infer further, we fix time t and distance z to see the role of parameters α, β and their impact on rogue waves in the following part.

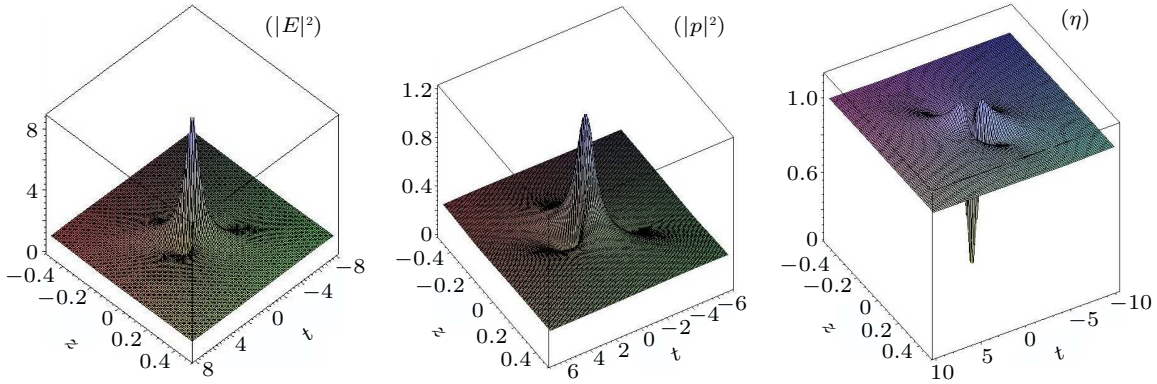


Fig. 10. (color online) Rogue wave solution (E, p, η) of the H-MB equations when $\omega = 1, d = 1, n_1 = 1, \alpha_1 = 1, \beta_1 = 1, \alpha = 2, \beta = -1$.

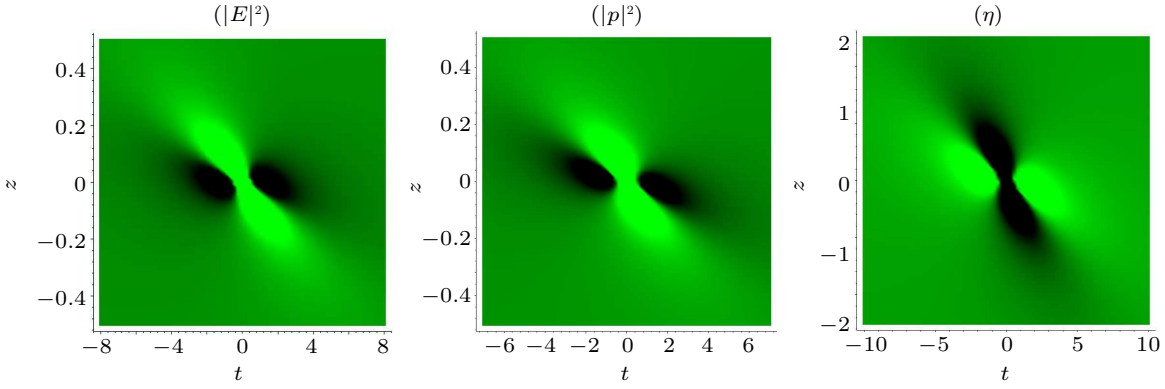


Fig. 11. (color online) Rogue wave solution (E, p, η) of the H-MB equation when $\omega = 1, d = 1, n_1 = 1, \alpha_1 = 1, \beta_1 = 1, \alpha = 2, \beta = -1$.

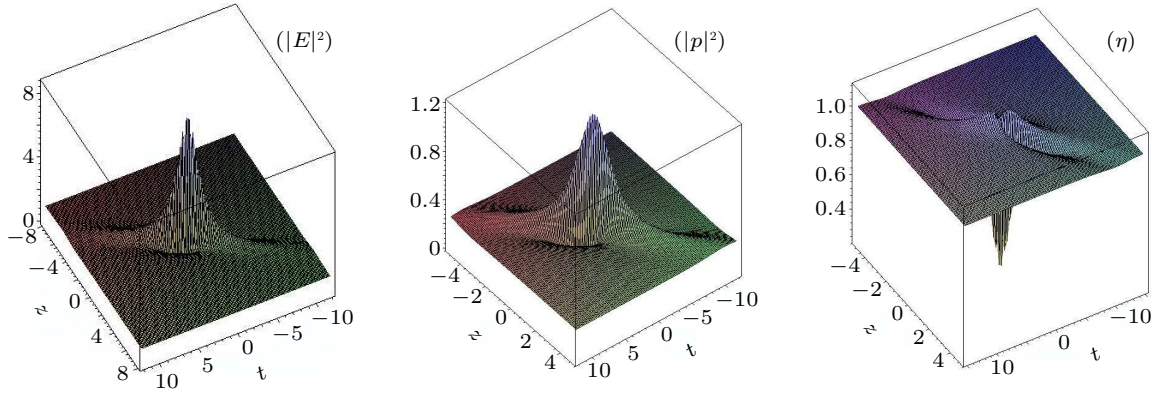


Fig. 12. (color online) Rogue wave solution (E, p, η) of the NLS-MB equations when $\omega = 1$, $d = 1$, $n_1 = 1$, $\alpha_1 = 1$, $\beta_1 = 1$, $\alpha = 1$, $\beta = 0$.

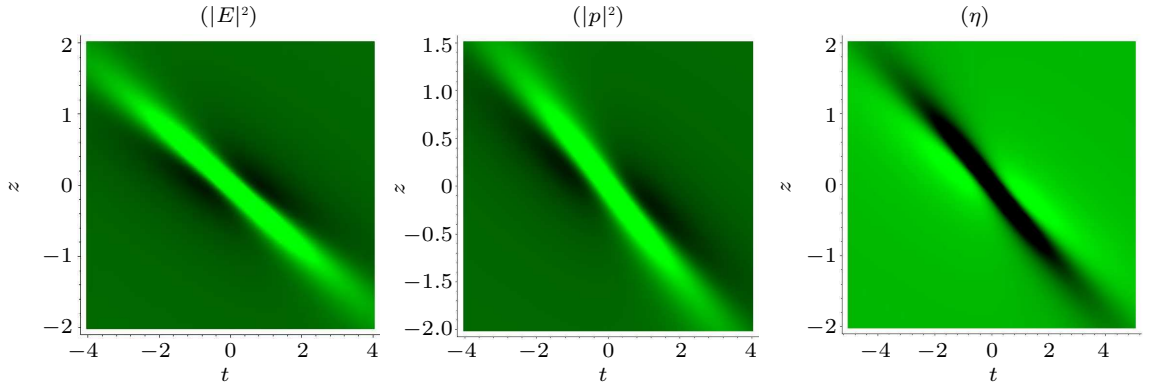


Fig. 13. (color online) Rogue wave solution (E, p, η) of the NLS-MB equations when $\omega = 1$, $d = 1$, $n_1 = 1$, $\alpha_1 = 1$, $\beta_1 = 1$, $\alpha = 1$, $\beta = 0$.

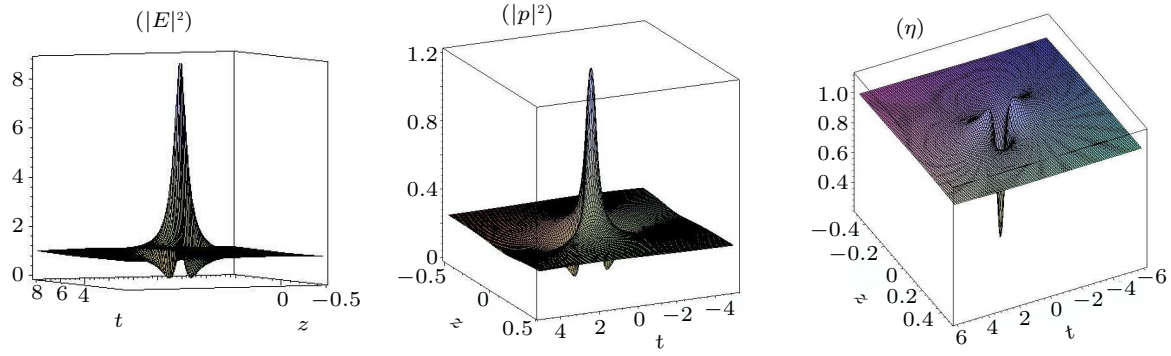


Fig. 14. (color online) Rogue wave solution (E, p, η) of the CMKdV-MB equation when $\omega = 1$, $d = 1$, $n_1 = 1$, $\alpha_1 = 1$, $\beta_1 = 1$, $\alpha = 0$, $\beta = 1$.

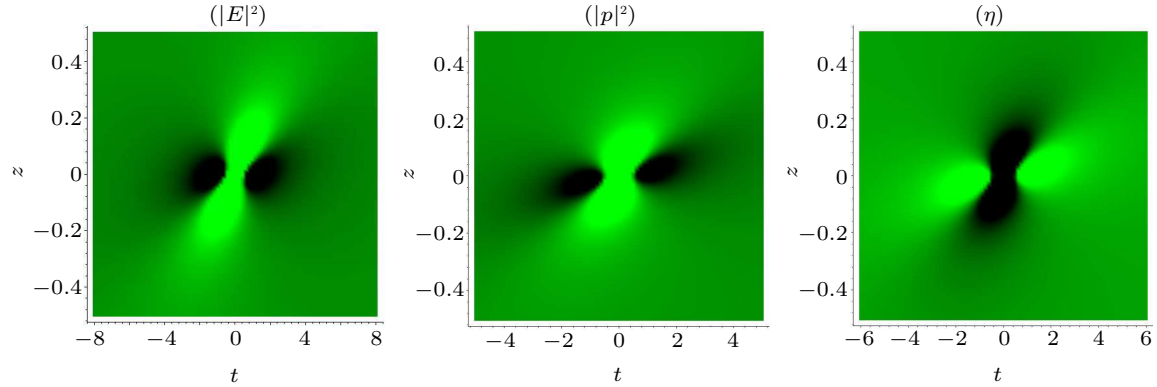


Fig. 15. (color online) Rogue wave solution (E, p, η) of the CMKdV-MB equation when $\omega = 1$, $d = 1$, $n_1 = 1$, $\alpha_1 = 1$, $\beta_1 = 1$, $\alpha = 0$, $\beta = 1$.

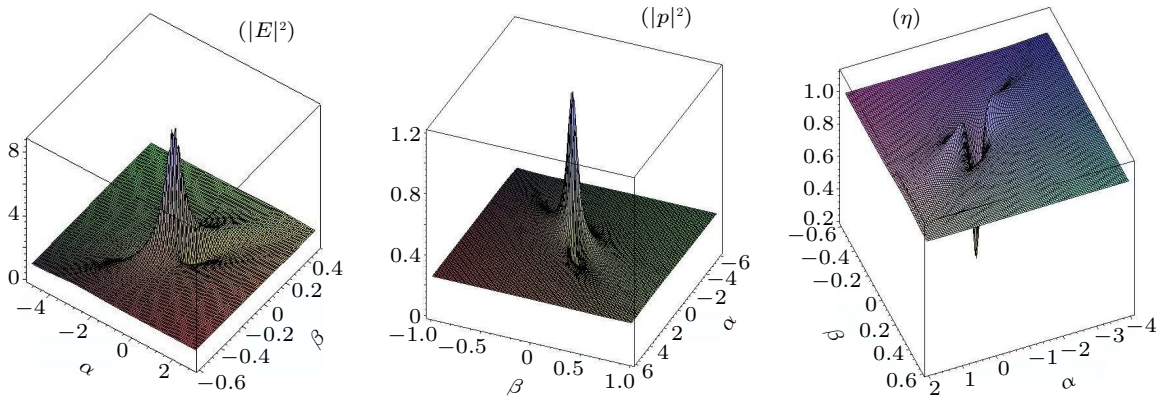


Fig. 16. (color online) Rogue wave solution (E, p, η) of the H-MB equation when $\omega = 1$, $d = 1$, $n_1 = 1$, $\alpha_1 = 1$, $\beta_1 = 1$, $t = 1$, $z = 1$.

We keep the parameters α and β as arbitrary parameters and choose $\omega = 1$, $d = 1$, $n_1 = 1$, $\alpha_1 = 1$, $\beta_1 = 1$, $t = 1$, $z = 1$, the solutions of $E_{r\alpha\beta}$ become

$$E_{r\alpha\beta} = \mathrm{e}^{-\mathrm{i}(4\beta+\alpha+1)}\Big(\frac{10-\mathrm{i}(240\beta-20\alpha+2)}{17+46\alpha+1800\beta^2+50\alpha^2-480\alpha\beta-120\beta}-1\Big). \tag{20}$$

This is also rogue wave whose graph is portrayed in Fig. 16 which also include graphs of $(p_{r\alpha\beta}, \eta_{r\alpha\beta})$. The above results clearly indicate that modification of the physical parameters α and β can be used to design experimental results.

From the above discussion, one can easily conclude that E and p are bright rogue waves, meanwhile η is a dark rogue wave.

6. Conclusion and discussions

In this paper, we described soliton solutions, the breather solutions, and rogue wave of the H-MB equations using Darboux transformation (it will be published in another mathematical way because of being too tedious) from trivial seed solutions and periodic seed solutions. The rogue waves show very nice characters which might attract physicists to observe it in experiment with higher-order optical effects in the femtosecond regime. In addition to soliton solutions, we have also constructed positon and rogue wave solutions. Meanwhile, we also observed the phase change of these solutions while comparing them with an un-doped two-level system. It is interesting to explore further physical interpretations and observations of higher-order positon solutions, higher-order rogue waves solutions and their applications in physics, in particular, a possible connection between these solutions and super-continuum generation in optical systems through higher-order soliton fission, etc. The work is still in progress.

References

[1] Agrawal G P 2006 *Nonlinear Fibre Optics* (San Diego: Academic Press)

[2] Huang G X 2001 *Chin. Phys.* **10** 418

[3] Zheng C L, Zhang J F, Wu F M, Sheng Z M and Chen L Q 2003 *Chin. Phys.* **12** 1009

[4] Hasegawa A and Matsumoto M 2003 *Optical Solitons in Fibres* (Berlin: Springer-Verlag)

[5] Porsezian K and Kuriakose V C 2009 *Solitons in Nonlinear Optics: Advances and Applications — European Journal of Physics Special Topics* (Berlin: Springer-Verlag)

[6] Akhmediev N N and Ankiewicz A 1997 *Solitons* (London: Chapman Hall)

[7] Taylor J R 1992 *Optical Solitons: Theory and Experiment* (Cambridge: Cambridge University Press)

[8] Abdullaev F, Darmanyan S and Khabibullaev P 1993 *Optical Solitons: Springer Series in Nonlinear Dynamics* (Berlin: Springer-Verlag)

[9] Abdullaev F 1994 *Theory of Solitons in Inhomogeneous Media* (New York: John Wiley)

[10] Kivshar Y S and Agrawal G P 2003 *Optical Solitons: From Fibers to Photonic Crystals* (San Diego: Academic Press)

[11] Kharif C and Pelinovsky E 2003 *Eur. J. Mech. B: Fluids* **22** 603

[12] Kharif C, Pelinovsky E and Slunyaev A 2009 *Rogue Waves in the Ocean* (Berlin: Springer)

[13] Akhmediev N, Ankiewicz A and Taki M 2009 *Phys. Lett. A* **373** 675

[14] Akhmediev N, Soto-Crespo J M and Ankiewicz A 2009 *Phys. Lett. A* **373** 2137

[15] Osborne A 2010 *Nonlinear Ocean Waves and the Inverse Scattering Transform* (New York: Elsevier)

[16] Bludov Yu V, Konotop V V and Akhmediev N 2009 *Phys. Rev. A* **80** 033610

[17] Wen L, Li L, Li Z D, Song S W, Zhang X F and Liu W M 2011 *Eur. Phys. J. D* **64** 473

[18] Ruderman M S 2010 *Eur. Phys. J. Special Topics* **185** 57

[19] Moslem W M, Shukla P K and Eliasson B 2011 *Europhys. Lett.* **96** 25002

[20] Yan Z Y 2011 *Phys. Lett. A* **375** 4274

[21] Efimov V B, Ganshin A N, Kolmakov G V, McClintock P V E and Mezhov-Deglin L P 2010 *Eur. Phys. J. Special Topics* **185** 181

[22] Efimov V B, Ganshin A N, Kolmakov G V, McClintock P V E and Mezhov-Deglin L P 2011 *Marrakesh Morocco Mar.* 20–23

[23] Solli D R, Ropers C, Koonath P and Jalali B 2007 *Nature* **450** 1054

[24] Kibler B, Fatome J, Finot C, Millot G, Dias F, Genty G, Akhmediev N and Dudley J M 2010 *Nat. Phys.* **6** 790

[25] Peregrine D H 1983 *J. Austral. Math. Soc. B* **25** 16

[26] Ankiewicz A, Soto-Crespo J M and Akhmediev N 2010 *Phys. Rev. E* **81** 046602

[27] Tao Y S and He J S 2012 *Phys. Rev. E* **85** 026601

[28] Xu S W, He J S and Wang L H 2011 *J. Phys. A: Math. Theor.* **44** 305203

[29] Xu S W and He J S 2012 *J. Math. Phys.* **53** 063507

[30] Ankiewicz A, Akhmediev N and Soto-Crespo J M 2010 *Phys. Rev. E* **82** 026602

[31] Guo B L and Lin L M 2011 *Chin. Phys. Lett.* **28** 110202

[32] Baronio F, Degasperis A, Conforti M and Wabnitz S 2012 *Phys. Rev. Lett.* **109** 044102
[33] Zhai B G, Zhang W G, Wang X L and Zhang H Q 2012 *Nonlinear Analysis: Real World Applications* **14** 14
[34] Yang G Y, Li L and Jia S T 2012 *Phys. Rev. E* **85** 046608
[35] Hasegawa A and Tappert F 1973 *Appl. Phys. Lett.* **23** 142
[36] McCall M and Hahn E L 1967 *Phys. Rev. Lett.* **18** 908
[37] Maimistov A I and Manykin E A 1983 *Sov. Phys. JETP* **58** 6851994
[38] Nakazawa M, Kimura Y, Kurokawa K and Suzuki K 1992 *Phys. Rev. A* **45** R23
[39] Nakazawa M, Suzuki K, Kimura Y and Kubota H 1992 *Phys. Rev. A* **45** R2682
[40] Tiofack C G L, Ekogo T B, Mohamadou A, Porsezian K and Kofane T C 2010 *J. Opt.* **12** 085202
[41] He J S, Cheng Y and Li Y S 2002 *Commun. Theor. Phys.* (Beijing, China) **38** 493
[42] He J S, Xu S W and Porseizan K 2012 *J. Phys. Soc. Jpn.* **81** 033002
[43] Nakkeeran K and Porsezian K 1995 *J. Phys. A: Math. Gen.* **28** 3817
[44] Porsezian K and Nakkeeran K 1995 *J. Mod. Opt.* **43** 693
[45] Kodama Y 1985 *Phys. Lett. A* **112** 193
[46] Hirota R 1973 *J. Math. Phys.* **14** 805
[47] Porsezian K, Hasegawa A, Serkin V N, Belyaeva T L and Ganapathy R 2007 *Phys. Lett. A* **361** 504
[48] Porsezian K and Nakkeeran K 1995 *Phys. Rev. Lett.* **74** 2941
[49] Matveev V B and Salle M A 1991 *Darboux Transformations and Solitons* (Berlin: Springer)
[50] He J S, Zhang L, Cheng Y and Li Y S 2006 *Sci. China A* **12** 1867